Finite Set Model Predictive Control of PWM AC/DC Converter with Virtual-Flux Estimation under Grid Imbalance

Imad Merzouk[1*], Khansa Bdirina[1], M. L. Bendaas[2]
1- Applied Automation and Industrial Diagnostic Laboratory, Faculty of Technology, University of Djelfa, Algeria.
Email: imadmer@yahoo.fr (Corresponding author)
2- Department of Technology, University of Batna, Algeria.

Received: June 2018 Revised: September 2018 Accepted: December 2018

ABSTRACT:
The aim of this research is to improve the quality of input current for AC/DC PWM converter, in case of grid imbalance with high dynamic transient. This can be achieved by joining compensating power with finite set model predictive control (FSMPC) based on voltage sensor-less technique. The control scheme proposed in this paper is divided into two steps. First, a double second order generalized integrator is used to estimate the virtual-flux and separate sequences of grid current and then the compensating power necessary to obtain sinusoidal input current is calculated. In the second step, the current is regulated via FSMPC, where, the switching state is determined directly. MATLAB/Simulink is selected to simulate and verify the effectiveness of the proposed control scheme; with and without virtual flux estimation. Simulation results are compared to confirm the validity of the algorithm.

KEYWORDS: AC/DC PWM Converter, Finite Set Model Predictive Control, Virtual Flux, Compensating Power, Grid Imbalance.

1. INTRODUCTION

PWM AC/DC converter has much interest in last few years due to its necessity in various applications such as grid integrated power conversion systems, wind energy conversion system (WECS), HVDC transmission and many other applications [1]. It offers sinusoidal current unity power factor, smooth and controllable dc link voltage, reversible active and reactive power flow, high efficiency and reliability and notably grid fault capability [2].

In grid integrated systems, unbalanced grid voltage is the most common issue that affects the global system functioning [3, 4]. Such perturbation affects the performance of the converter and brings some deterioration in grid currents and dc link voltage. [5] Researchers are interested in developing new algorithms to control the PWM AC/DC converter under grid unbalance to improve its performance [6].

First a modified voltage-oriented control (VOC) is proposed in the work of [3], [7]. The modified VOC can improve both the quality of grid currents and dc-link voltage. Currents become sinusoidal but still unbalanced and the tuning of gain regulators limits the use of this method.

Modified direct power control (DPC) is an alternative to VOC. It is simple to implement, robust and it does not need a PI regulator [8, 9]. It can achieve one of these goals at a time: balanced and sinusoidal grid currents, smooth active power or oscillation free reactive power. Depending on the equations of active and reactive powers in the ideal and unbalanced state and based on the chosen goal, the compensating powers are calculated and injected to the referencing one.

The development of microcontrollers allows the use of new modern control techniques in power electronics systems. Finite set model predictive control (FSMPC) is one of the new approaches developed recently to control power converters [10, 11]. It has several advantages; it is simple and robust and it gives fast dynamic response for the system [12].

At the same time, voltage-sensor-less operating control took great importance to avoid the additional sensor cost, complexity and to increase the reliability of overall system [13]. Virtual flux technique is the most responding for voltage sensor-less control. In general, filters are used to estimate virtual flux [14, 15]. But under unbalanced conditions, where the separating positive and negative sequences are needed, cascading filter must be used [16]. However, it creates more time delay and reduces the accuracy. Double second order generalized integrator (DSOGI) is a good alternative to remove the drawback of cascading filter, it could estimate the virtual-flux and separate sequences of virtual flux and grid current [17].

Combining compensating power technique with FSMPC and virtual flux based on voltage-sensor-less technique would achieve the best results. This paper proposes a new voltage-sensor-less control scheme for PWM AC/DC converter under the grid unbalance to get sinusoidal and symmetrical grid current with fast dynamic response. For that, the referencing currents are calculated via instantaneous power theory and then the switching state that should be applied to semiconductor device are determined directly by minimizing the cost function in finite set model predictive control block.

The manuscript is subdivided in three sections. After presenting the converter model and MPC strategy in the first section, the control law is extracted in the case of voltage sensor-less predictive control in the second section. The last section is devoted to simulation results and comparative study, where control scheme is verified by numerical simulation using MATLAB-Simulink environment.

2. CONTROL THEORY

The overall section of the control theory is divided into four sub sections. In the first section, a detailed model of PWM AC/DC converter in stationary rotating frame is given, after that the used method of estimation of virtual flux based on DSOGI and the separation of positive and negative sequence are discussed in the second section. The third section is reserved to calculate the referencing current to be applied to finite set model predictive current control block with unbalance compensation. In the last sub section, predictive control with cost function is realized.

2.1. System Modeling

The topology of the three-phase grid-connected converters is shown in Fig. 1.

Depending on the structure of PWM converter shown in Fig. 1 and using Clark transformation, we find a mathematical model in αβ stationary coordinate frame of PWM converter as follows:

$$\begin{cases} L\frac{dI_\alpha}{dt} = E_\alpha - Ri_\alpha - V_\alpha \\ L\frac{dI_\beta}{dt} = E_\beta - Ri_\beta - V_\beta \end{cases} \quad (1)$$

Where:

E_α, E_β: Source voltage in rotating frame.

V_α, V_β: Converter terminals voltage.

I_α, I_β: Line current.

L, R: Input filter inductance and resistance.

The converter voltage terminal can be estimated using the measured dc-link voltage and the switching frequency according to (2):

$$\begin{cases} V_\alpha = v_{dc}S_\alpha \\ V_\beta = v_{dc}S_\beta \end{cases} \quad (2)$$

S_α, S_β: switching function

v_{dc}: DC-link voltage

Substituting (2) in (1) we find:

$$\begin{cases} L\frac{dI_\alpha}{dt} = E_\alpha - Ri_\alpha - v_{dc}S_\alpha \\ L\frac{dI_\beta}{dt} = E_\beta - Ri_\beta - v_{dc}S_\alpha \end{cases} \quad (3)$$

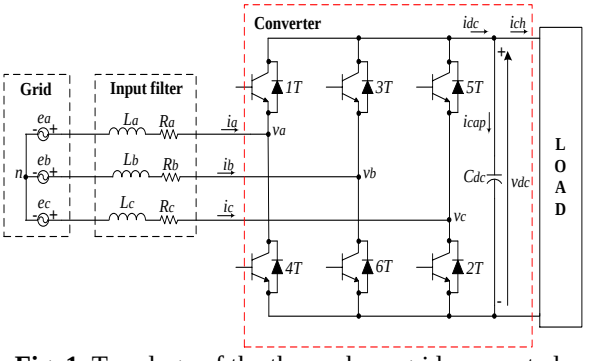

Fig. 1. Topology of the three-phase grid-connected converter.

2.2. Virtual Flux Estimation

For sensor-less AC-voltage control of AC/DC PWM converter virtual flux concept is the most adopted method in literature. Therefore, we can benefit from two main advantages: cost reduction by reducing the number of sensors and natural filtering of line voltage harmonics.

By integrating the AC-voltage, the virtual flux can be obtained as follows:

$$\psi_{\alpha\beta} = \int E_{\alpha\beta}dt \quad (4)$$

Replacing the AC-voltage by its equivalent value extracted from the AC-side converter model we get:

$$\psi_{\alpha\beta} = LI_{\alpha\beta} + \int\left(Ri_{\alpha\beta} + V_{\alpha\beta}\right)dt \quad (5)$$

Under unbalanced conditions the virtual flux (VF) is decomposed on the sum of positive and negative sequences according to symmetrical component theory. So, to separate the instantaneous values of positive and negative quantities usually cascading filter-method is used. Unfortunately, this method suffers from several disadvantages (time delay, sensitivity to grid frequency variation, complex structures and relatively slow transient response). The Double Second Order multiple Generalized Integrator (DSOGI) is one of the more feasible solutions proposed so far in the literature for its

good results in terms of the accuracy and its capability for grid synchronization [16].

$$D(s) = \frac{U(s)}{U(s)} = \frac{k.\omega s}{s^2+k.\omega.s+\omega^2} \quad (6)$$

$$Q(s) = \frac{U(s)}{U(s)} = \frac{k.\omega'^2}{s^2+k.\omega.s+\omega'^2} \quad (7)$$

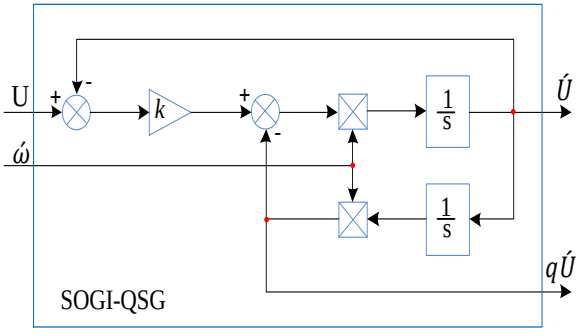

Fig. 2. Structure of SOGI-QSG.

The structure of (SOGI) is given in Fig. 2. where the constant K is the damping factor of the filter that determines the performance and the dynamic response of the SOGI k is selected as k =$\sqrt{2}$ for optimum value time response and overshoot.

Taking advantage of the two output of SOGI, the first which is in phase and has the same amplitude as the input; and the second which is shifted by 90 degrees from the input while conserving the same amplitude. Therefore, we can use the SOGI to integrate (equation 5) and consequently estimate the virtual flux. In addition, we can separate the positive and negative sequences of the virtual flux using both outputs of the SOGI and by a Positive-Negative-Sequence Calculator (PNSC) equations (8,9,10) [17].

$$U_{\alpha\beta} = [T_{\alpha\beta}]u_{abc} / \ [T_{\alpha\beta}] = \frac{2}{3}\begin{bmatrix} 1 & \frac{-1}{2} & \frac{-1}{2} \\ 0 & \frac{\sqrt{3}}{2} & \frac{-\sqrt{3}}{2} \end{bmatrix} \quad (8)$$

$$U^{+}_{\alpha\beta} = \frac{1}{2}\begin{bmatrix} 1 & -q \\ q & 1 \end{bmatrix} U_{\alpha\beta} \quad (9)$$

$$U^{-}_{\alpha\beta} = \frac{1}{2}\begin{bmatrix} 1 & q \\ -q & 1 \end{bmatrix} U_{\alpha\beta} \quad (10)$$

$q = e^{-j(\frac{\pi}{2})}$. is a lagging phase shift operation PNSC structure is illustrated in Fig.3.

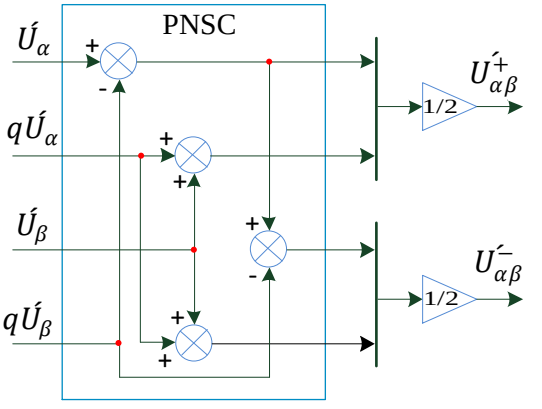

Fig.3. Structure of PNSC.

The complete structure of virtual flux estimation with sequences separation is illustrated in Fig. 4.

2.3. Unbalance Compensation Technique

With the virtual flux approach active and reactive powers can be calculated from [14]:

$$\begin{cases} P = \frac{3}{2}\omega(\psi_\alpha I_\beta - \psi_\beta I_\alpha) \\ Q = -\frac{3}{2}\omega(\psi_\alpha I_\alpha + \psi_\beta I_\beta) \end{cases} \quad (11)$$

Using symmetrical component theory

$$\begin{cases} P = \frac{3}{2}\omega(\psi^+_\alpha I^+_\beta - \psi^+_\beta I^+_\alpha + \psi^-_\alpha I^-_\beta - \psi^-_\beta I^-_\alpha + \psi^+_\alpha I^-_\beta - \psi^+_\beta I^-_\alpha + \psi^-_\alpha I^+_\beta - \psi^-_\beta I^+_\alpha) \\ Q = -\frac{3}{2}\omega(\psi^+_\alpha I^+_\alpha + \psi^+_\beta I^+_\beta + \psi^-_\alpha I^-_\alpha + \psi^-_\beta I^-_\beta + \psi^+_\alpha I^-_\alpha + \psi^+_\beta I^-_\beta + \psi^-_\alpha I^+_\alpha + \psi^-_\beta I^+_\beta) \end{cases} \quad (12)$$

For symmetrical and harmonic free components of line current we must impose the negative component of current in the equations (12) zero so we get:

$$\begin{cases} P = \frac{3}{2}\omega(\psi^+_\alpha I^+_\beta - \psi^+_\beta I^+_\alpha + \psi^-_\alpha I^+_\beta - \psi^-_\beta I^+_\alpha) \\ Q = -\frac{3}{2}\omega(\psi^+_\alpha I^+_\alpha + \psi^+_\beta I^+_\beta + \psi^-_\alpha I^+_\alpha + \psi^-_\beta I^+_\beta) \end{cases} \quad (13)$$

Compared to equations (13) and (11) we get the compensation power as:

$$\begin{cases} P_{comp} = \frac{3}{2}\omega(\psi^-_\alpha I^+_\beta - \psi^-_\beta I^+_\alpha) \\ Q_{comp} = -\frac{3}{2}\omega(\psi^-_\alpha I^+_\alpha + \psi^-_\beta I^+_\beta) \end{cases} \quad (14)$$

Then the reference currents values can be easily deducted and given in the equation bellow

$$\begin{cases} I_{\alpha ref} = \frac{2}{3\Delta}\omega\left(\psi_\alpha(P_{ref}+P_{comp}) + \psi_\beta(Q_{ref}+Q_{comp})\right) \\ I_{\beta ref} = \frac{2}{3\Delta}\omega\left(\psi_\beta(P_{ref}+P_{comp}) - \psi_\alpha(Q_{ref}+Q_{comp})\right) \end{cases} \quad (15)$$

Where, $\Delta = \omega^2(\psi^2_\alpha + \psi^2_\beta)$. The subscript (*ref*) means reference value.

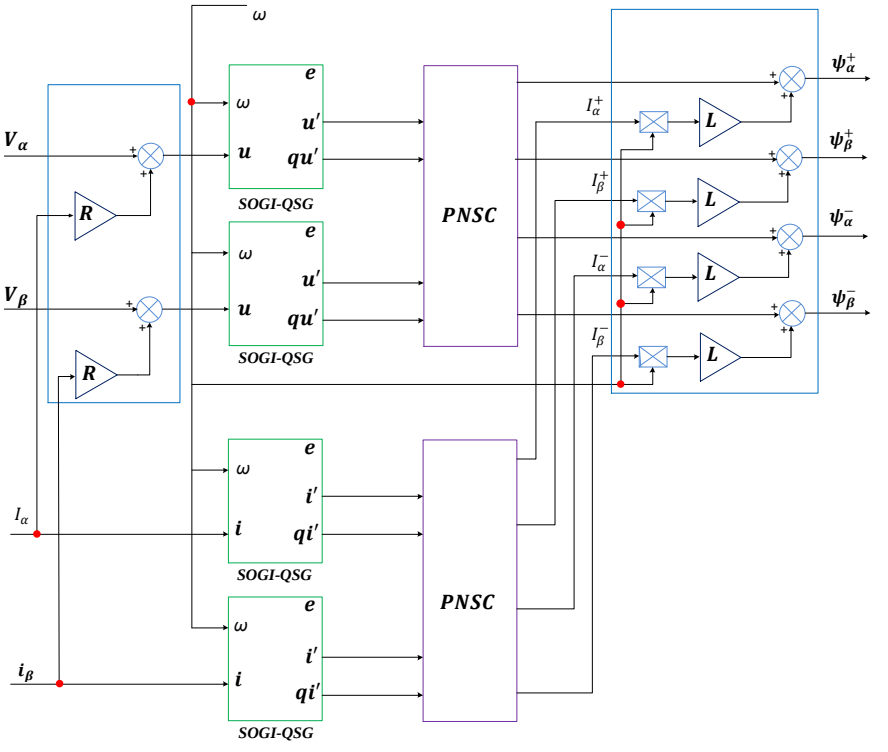

Fig. 4. Complete structure of virtual flux estimation with sequence separation.

2.4. Predictive Current Control

In order to estimate the future value of measured current, the discrete time model of the system is needed.

Using Euler approximation [18]:

$$\frac{di}{dt} = \frac{i(k+1)-i(k)}{T} \tag{16}$$

Substituting (16) in (3) we find the discrete model:

$$\begin{bmatrix} I_\alpha(k+1) \\ I_\beta(k+1) \end{bmatrix} = \begin{bmatrix} 1-\frac{RT}{L} & 0 \\ 0 & 1-\frac{RT}{L} \end{bmatrix} \begin{bmatrix} I_\alpha(k) \\ I_\beta(k) \end{bmatrix} + \begin{bmatrix} \frac{T}{L} & 0 \\ 0 & \frac{T}{L} \end{bmatrix} \begin{bmatrix} E_\alpha - V_{dc}(k)S_\alpha(k) \\ E_\beta - V_{dc}(k)S_\beta(k) \end{bmatrix} \tag{17}$$

According to (17) we can predict the future value of line current using actual values of line current, source voltage, DC link voltage and switching function.

In this work our main objective is current tracking of grid current. So the cost function is selected as:

$$g(k) = \lambda\left[I_{\alpha ref}(k) - I_\alpha(k+1)\right] + \gamma\left[I_{\beta ref}(k) - I_\beta(k+1)\right] \tag{18}$$

Where, λ, γ are the weighing coefficients of line currents.

After sampling the line current and predicting the future values, these values are compared with extrapolated referencing currents. In this paper we assume that the reference current is not sufficiently changed in one sampling interval, therefore, $I_{ref}(k+1) = I_{ref}(k)$. By assuming this, a one sample delay is caused in the reference tracking, which is acceptable if a high sampling frequency is considered [19].

Then the cost function is calculated depending on eight possible cases. The switching state, among the eight possible states, which gives the minimum cost function is chosen and applied to the PWM rectifier gating terminals.

The control diagram of the proposed control scheme is drawn in the Fig. 5. Two cascading control loops are distinguished, the role of the outer loop is to regulate the level of Dc voltage via a PI regulator and consequently deliver the referencing active power which is used with the reactive power to calculate the current. The measured and referencing currents are the entrance of the inner loop where the switching state is determined via model predictive control.

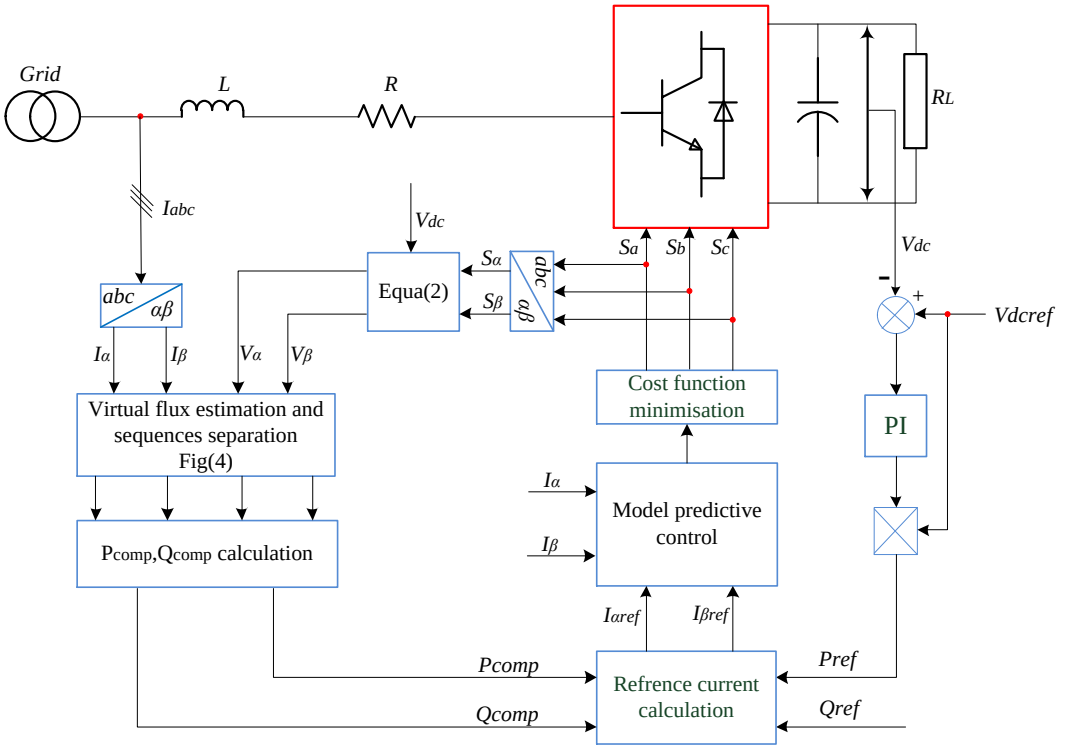

Fig. 5. Control diagram of the proposed MPC.

3. SIMULATION AND INTERPRETATION

In order to investigate the effectiveness of the mentioned approach of voltage sensor-less control, the control scheme in Fig. 5 was simulated using MATLAB/ Simulink environment. The converter parameters are given in Table 1. The design of model predictive controller is based on the discrete model. The general control objective is to extract the switching state that allows to track the reference current, using cascade structure.

Table 1. Power circuit parameters.

Items	Symbol	Value
Input filter inductance	L	$12mH$
Input filter resistance	R	0.3Ω
DC-bus capacitor	C_{dc}	$500\mu F$
Load resistance	R_L	200Ω
DC voltage	V_{dc}	$400V$
AC source voltage	e	160
Sampling time	T_s	$10\mu S$

In order to have a comparative benchmark result for the data obtained using a proposed voltage-sensor-less compensating control scheme under unbalanced supply conditions, the control scheme was simulated under balanced case too.

3.1. Operation under Balanced Grid

In this case, the grid voltage is assumed to be balanced. But, when the simulation reaches a steady state, steps are applied on the reference of DC-link voltage, the reference of reactive power, the value of resistive load and finally in the input voltage magnitude. The results are presented in Figs. 6-10.

At t=0.5 s, a 10 % step is first applied to the reference of the DC-link voltage (increase from 400V to 440V). The DC voltage stabilizes to the new reference on approximately 0.05s as shown Fig. 6. With this change, the active power exchanged with the grid was increased too to assure the required power requested at the output of the converter as observed in Fig. 7. The reactive power stays unchanged.

At t= 0.7, the second step was introduced where the reference reactive power was increased from 0Var to 1000 Var. The reactive power is smooth and follows its reference with a good accuracy. With the change of reactive power, the active power stays unchanged. So, the decoupled control of active and reactive power is assured. We can also observe that the measured and estimated active and reactive powers are superposed so the sensor-less voltage control works well.

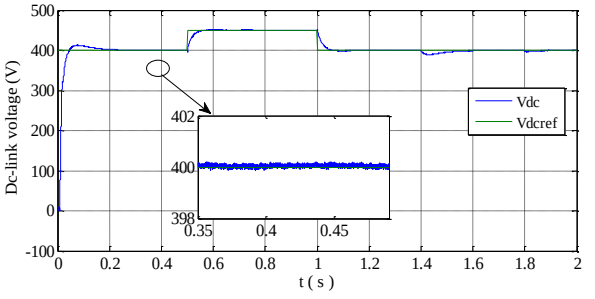

Fig. 6. Dc-link voltage.

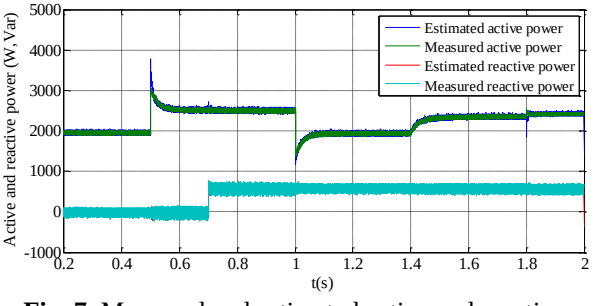

Fig. 7. Measured and estimated active and reactive power.

The input current in Fig. 8 follows its sinusoidal reference during both steady state and transient state with a change of amplitude. The THD of current is about 3%. The response of input current to all imposed steps is stable and rapid, this means that the inner predictive loop has high control performances. Input current and voltage are both illustrated in Fig. 9. It is clearly observed that the unity power factor is granted when the reference reactive power is 0, and the voltage and current waveforms are not in-phase with the change of the reactive power value.

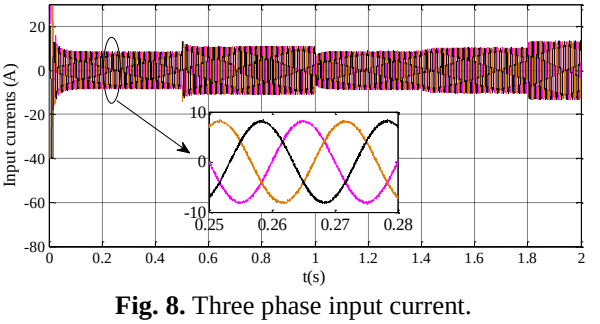

Fig. 8. Three phase input current.

Deactivating the steps applied on the DC voltage reference at t=1s, the two last steps (the value of resistive load and the input voltage magnitude) are applied later in t= 1.4 s and t=1.8 s consecutively. When the load decreases (from 100Ω to 80Ω), the active power increases as well as the amplitude of the input current, however, the DC voltage decreases slightly and then returns to its reference and the system stays stable.

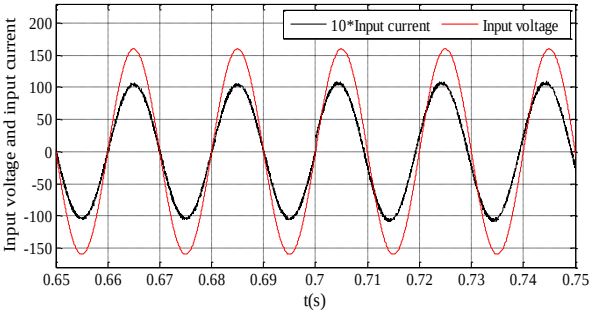

Fig. 9. Input current and grid voltage.

Fig. 10 shows the wave of the measured and estimated α/β component of grid voltage. It can be clearly noticed that the measured and the estimated quantities are coincided and after the voltage sag (15% from the magnitude) the SOGI tracks the new value of voltage within 1/4 of grid period.

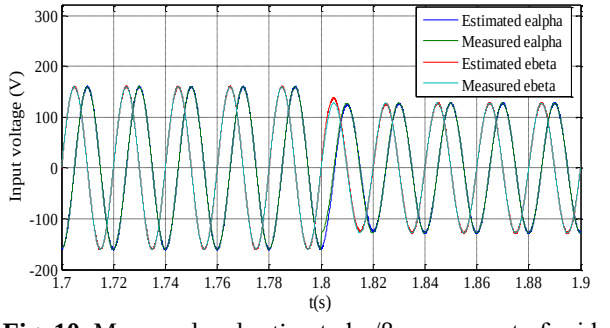

Fig. 10. Measured and estimated α/β component of grid voltage.

3.2. Operation under Unbalanced Grid

The simulation performed in the previous subsection allows us to examine the system response to steps on the regulators reference. In this subsection, we will investigate the dynamic response of the system under unbalance perturbation in the AC grid.

The system was simulated under voltage change from balanced case to one phase unbalanced case at time t=0.4 s, after 0.05 s the compensating active and reactive power are injected (equation 14). The control scheme can ensure a sinusoidal and balanced current under balanced AC grid. The presence of an unbalance creates undesired pulsation in the Dc-link voltage. The reflected pulsations combined with the fundamental of the space vector modulation generate law order harmonics in input current especially third and fifth harmonics. Active and reactive powers become fluctuated but unchanged of the mean value. The injected compensating power can effectively enhance the wave form of input current with reducing unbalance degrees and eliminating the harmonics.

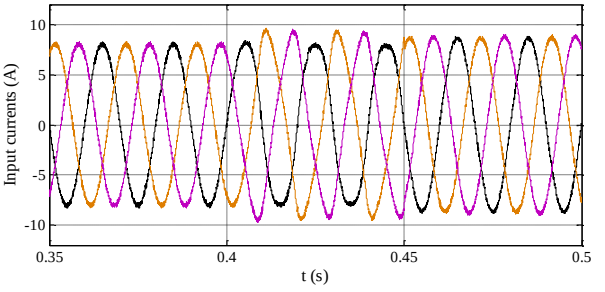

Fig. 11. Three phase input current.

As demonstrate in Fig. 12. the d-q axis input currents are smooth under ideal grid but the unbalance creates ripples in dq axis currents resulting in imbalance and harmonics in three phases frame. After introducing compensating techniques, those ripples were reduced and thus the wave form of currents was improved.

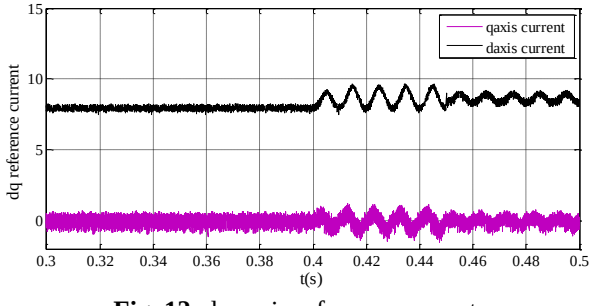

Fig. 12. d-q axis reference current.

The measured and estimated active and reactive powers are coinciding under balanced or unbalanced operations as seen in Fig .13 so the DSOGI can estimate the active and reactive powers with infinite precision.

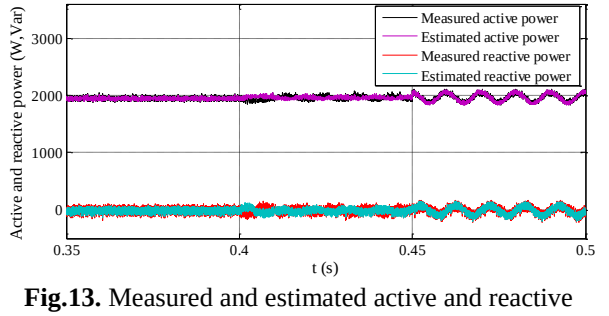

Fig.13. Measured and estimated active and reactive power.

From Fig. 15, the positive αβ components of virtual flux are perfectly sinusoidal and the negative αβ components are null under balanced operation. When an imbalance occurs, the value of the negative sequence of the virtual flux changes rapidly to a sinusoidal signal. Between the instants t=0.4 and t=0.45, it can be seen that there is some deterioration in the wave form of negative sequence of virtual flux due to the harmonics in the input current. But, after the compensating techniques were introduced, the harmonics in input current were removed which improved the quality of estimated virtual flux.

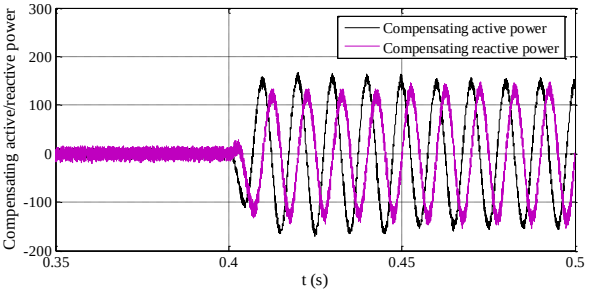

Fig. 14. Estimated active and reactive compensating powers.

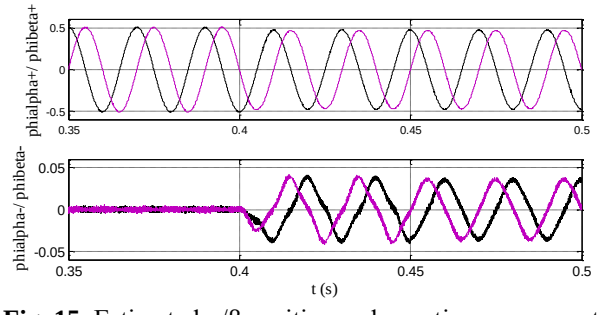

Fig. 15. Estimated α/β positive and negative component of virtual flux.

The measured and estimated input voltages are shown in Fig. 16. The deterioration in the negative sequence of virtual flux does not affect AC voltage estimation. The estimated and measured voltages are superposed and the SOGI can track any change in the AC grid with fast response and high accuracy.

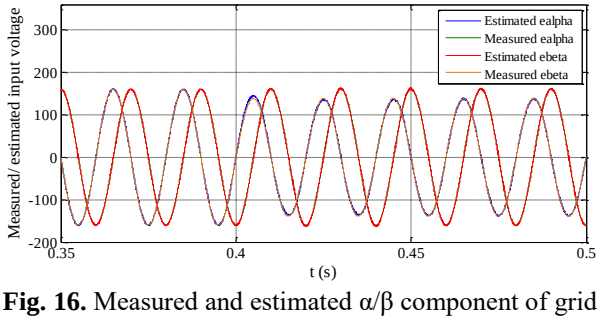

Fig. 16. Measured and estimated α/β component of grid voltage.

To quantify the enhancement in input current wave form, the THD of the current under three cases is shown: balanced case, unbalanced case without compensation and unbalanced case with compensation. It can be observed from Fig. 17 to 8.07 % in the second

case, where the third harmonic amplitude is about 8% of the fundamental magnitude. After the introduction of compensating power, the third harmonic amplitude is reduced to 0.1 % and the THD becomes 2.19 %.

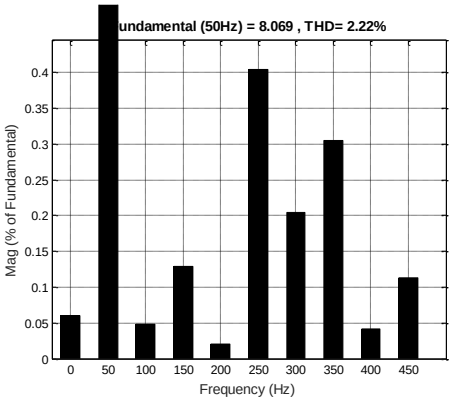

(a)

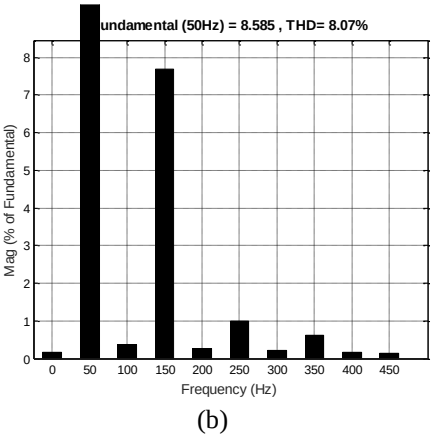

(b)

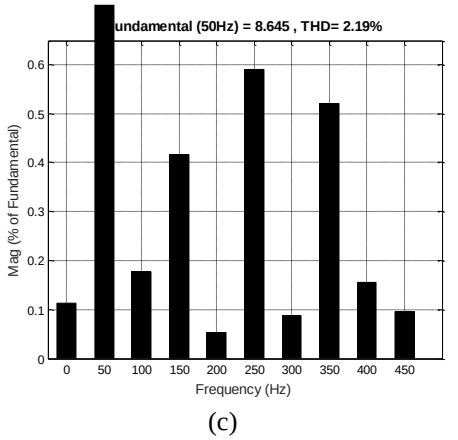

(c)

Fig. 17. THD of input current.

4. CONCLUSION

In this paper a voltage sensor-less control model predictive control scheme of AC/DC converter under unbalanced AC grid was studied. Virtual flux techniques were selected to estimate the input AC voltage using double second order generalized integrator (DSOGI) that allowed the estimation of grid voltage in balanced and unbalanced operation with high dynamics and accuracy. The whole control was subdivided into two sections. First, the referencing currents were calculated by the concept of compensating power to eliminate the effect of imbalance on input current waveforms. Second, the switching state was generated by optimizing the objective function. Several examinations of dynamic performance were performed and the simulation results achieved were very encouraging in terms of: stability, efficiency rapidity and accuracy. The input current was balanced and the THD was considerably reduced.

REFERENCES

[1] X. Xing, Ch. Zhang, J. He, A. Chen and Z. Zhang. **"Model Predictive Control for Parallel Three Level T-Type Grid-Connected Inverters in Renewable Power Generations".** *IET Renewable Power Generation.* Vol. 11 No. 11, pp. 1353-1363, DOI. 10.1049/iet-rpg.2016.0361, 2017.

[2] K. Kulikowski, A. Sikorski. **"New DPC Look-Up Table Methods for Three-Level AC/DC Converter".** *IEEE Transactions on Industrial Electronics*, Vol. 63, No. 12, pp. 7930- 7938, DOI. 10.1109/TIE.2016.2538208, 2016.

[3] Y. Suh, T. A. Lipo. **"Control Scheme in Hybrid Synchronous Stationary Frame for PWM AC/DC Converter under Generalized Unbalanced Operating Conditions".** *IEEE Transactions on Industry Applications*, Vol. 42, No. 3, pp. 825-835, DOI. 10.1109/TIA.2006.873673, 2006.

[4] Q. N. Trinh, P. Wang, and F. H. Choo., **"An Improved Control Strategy of Three-Phase PWM Rectifiers Under Input Voltage Distortions and DC-Offset Measurement Errors".** *IEEE Journal of Emerging and Selected Topics in Power Electronics*, Vol. 5, No. 3, pp. 1164-1176, DOI. 10.1109 /JESTPE .2017.2670229, 2017.

[5] L. Shang, D. Sun J. Hu. **"Sliding-Mode-Based Direct Power Control of Grid-Connected Voltage-Sourced Inverters Under Unbalanced Network Conditions".** *IET Power Electronics pp IET Power Electron*, Vol. 4, No. 5, pp. 570–579, DOI. 10.1049/ iet-pel.2010.0160, 2011.

[6] Y. Zhang, J. Gao, and Ch. Qu. **"Relationship between Two Direct Power Control Methods for PWM Rectifiers under Unbalanced Network",** *IEEE Transactions on Power Electronics*, Vol. 32, No. 5, pp. 4084 - 4094, DOI. 10.1109 /TPEL. 2016. 2593723, 2017.

[7] J. Hu, Y. He. **"Modeling and Control of Grid-Connected Voltage-Sourced Converters under Generalized Unbalanced Operation Conditions"**, *IEEE Transactions on Energy Conversion*, Vol. 23, No. 3, pp. 903-913, DOI. 10.1109/TEC.2008.921468, 2008.

[8] J. Eloy-Garcı´a, S. Arnaltes and J.L. Rodrı´guez-Amenedo., **"Direct Power Control of Voltage Source Inverters with Unbalanced Grid**

Voltages", *IET Power Electron*, Vol. 1, No. 3, pp. 395–407, DOI. 10.1049/iet-pel:20070042, 2008.

[9] Y. Zhang, Y. Peng, and Ch. Qu., **"Model Predictive Control and Direct Power Control for PWM Rectifiers with Active Power Ripple Minimization".** *IEEE Transactions on Industry Applications*, Vol. 52, No. 6, pp. 4909 - 4918, DOI. 10.1109/TIA.2016.2596240, 2016.

[10] H. A. Young, M. A. Perez, and J. Rodriguez, **"Analysis of Finite-Control-Set Model Predictive Current Control with Model Parameter Mismatch in a Three-Phase Inverter".** *IEEE Transactions on Industrial Electronics*, Vol. 63, No. 5, pp. 3100 - 3107, DOI. 10.1109/TIE.2016.2515072, 2016.

[11] N. Jin, Sh. Hu, Ch. Gan, and Zh. Ling, **"Finite States Model Predictive Control for Fault-Tolerant Operation of a Three-Phase Bidirectional AC/DC Converter Under Unbalanced Grid Voltages".** *IEEE Transactions on Industrial Electronics*, Vol. 65, No. 1, pp. 819 - 829, DOI. 10.1109/TIE. 2017. 2686 342, 2018.

[12] P. Falkowski, A. Sikorski. **"Finite Control Set Model Predictive Control for Grid-Connected AC-DC Converters with LCL Filter"**. *IEEE Transactions on Industrial Electronics*, Vol. 65, No. 4, pp. 2844-2852. DOI. 10.1109/TIE.2017.2750627, 2018.

[13] H. Yang, Y. Zhang, N. Zhang, P. D. Walker and J. Gao. **"A Voltage Sensorless Finite Control Set-Model Predictive Control for Three-Phase Voltage Source PWM Rectifiers".** *Chinese Journal of Electrical Engineering*, Vol. 2, Iss. 2, pp. 52 - 59, DOI. 10.23919/CJEE.2016.7933126, 2016.

[14] M. Malinowski, M. P. Kazmierkowski, S. Hansen, F. Blaabjerg, and G. D. Marques. **"Virtual Flux-Based Direct Power Control of Three-Phase Pwm Rectifiers".** *IEEE Trans. on Industry Applications*, Vol. 37, No. 4, pp. 1019–1027, DOI. 10.1109/28.936392, 2001.

[15] P. Antoniewicz, M. P. Kazmierkowski., **"Virtual Flux Based Predictive Direct Power Control of Ac/Dc Converters with On-Line Inductance Estimation,"** *IEEE Trans.on Industrial Electronics*, Vol. 55, No. 12, pp. 4381–4390, DOI. 10.1109/TIE. 2008.2007519, 2008.

[16] P. Rodríguez, A. Luna, I. Candela, R. Mujal, R. Teodorescu, and F. Blaabjerg., **"Multiresonant Frequency-locked Loop for Grid Synchronization of Power Converters Under Distorted Grid Conditions".** *IEEE Transactions on Industrial Electronics*, Vol. 58, No. 1, pp.127-138, DOI. 10. 1109/TIE.2010.2042420, 2011.

[17] J. A. Suul; A. Luna; P. Rodríguez and T. Undeland., **"Virtual-Flux-Based Voltage-Sensor-Less Power Control for Unbalanced Grid Conditions".** IEEE Transactions on Power Electronics, Vol. 27, No. 9, pp. 4071 - 4087, DOI. 10.1109/TPEL.2012.2190301, 2012.

[18] V. Kumar, P. Gaur and A. Prakash Mittal. **"Finite-State Model Redictive Control of NPC Inverter using Multi-Criteria Fuzzy Decision-Making".** *Int. Trans. Electrical. Energy. Systems*, Vol. 25, Iss 5, pp. 876–897, DOI. 10.1002/etep.1880, 2015.

[19] J. Rodríguez, P. C. Estay, Predictive Control of Power Converters and Electrical Drives., Iley, Chichester, West Sussex, UK; Hoboken, N.J.; 2012.